Quantitative interpretation of RASCAN holographic radar response from inclined plane reflectors by a theoretical model

L. Capineri, P. Falorni
Dipartimento Elettronica e Telecomunicazioni
Università di Firenze
Firenze, Italy
capineri@ieee.org pfalorni@gmail.com

V. Razevig
Remote Sensing Laboratory
Bauman Moscow State Technical University
Moscow, Russia
vrazevig@rslab.ru

M. Inagaki
Walnut Ltd
Saiwaicho, Tachikawa, Tokio, Japan
ina_mas@beige.plala.or.jp

T. Bechtel
Department of Earth and Environment
Franklin and Marshall College, Lancaster, PA, USA
tbechtel@fandm.edu

C. Windsor
116, New Road, East Hagbourne, OX11 9LD, UK
Colin.Windsor@ccfe.ac.uk

Abstract — **Holographic radar of RASCAN type provides an output signal that is amplitude-modulated by the phase variation between transmitted and received signals. In this work RASCAN radar response is compared with a model by several experiments performed in air with a 4GHz probe scanning a planar metallic reflector inclined at different angles. The radar response shows a series of dark and light stripes with spacing dependent on signal frequency and velocity, and reflector inclination angle. The model is used to interpret the amplitude variations as a function of probe position.**

Keywords-component; RASCAN, electromagnetic modeling, holographic radar, plane reflector, interference pattern.

I. INTRODUCTION

Holographic radar of RASCAN type produces grey scale images by scanning over objects of different shapes and materials **Errore. L'origine riferimento non è stata trovata.**. Standard imaging techniques from holographic data are not applicable in real lossy media because in this case refraction fringes are not extended enough and the information is degraded.

Experiments with holographic radar (4GHz RASCAN type) **Errore. L'origine riferimento non è stata trovata.Errore. L'origine riferimento non è stata trovata.** on inclined planar metal reflectors in air, have shown that in this case holographic radar produces images with alternating dark and light stripes that have been called the "zebra effect". The experiments pointed out that the zebra effect depends on the tilt angle of the inclined metal plate. This effect is visible also in real world investigations with holographic radar **Errore. L'origine riferimento non è stata trovata.**. For example, in the case of scanning the side part of a pillar, the iron reinforcement bars are revealed with the zebra effect. In this case, the metal bars are not parallel to the side of the pillar due to bad construction procedures.

This study is intended to apply a simple theoretical model to interpret or to predict the spatial distance of contrast maxima and minima related to the holographic radar wavelength. In this paper, a description of the model and the mathematical formulation is presented, followed by the validation of the model on RASCAN images acquired at various tilt angles.

II. EXPERIMENT DESCRIPTION

The experimental setup consists of a wooden scanning plane inclined at a given angle α over a horizontal aluminum plate, see Figure 1.

978-1-4244-4605-6/09/$25.00 ©2009 IEEE

Figure 1: picture of the experimental setup.

Although the RASCAN is designed for subsurface investigation of dielectric materials, we choose to operate our experiments in air to ensure a constant propagation velocity c and low medium attenuation. The scan lines are parallel to the x axis shown in Figure 1. The scanning plane was inclined at four different angles α equal to 10.4, 19.7 and 29.7 degrees.

The geometry of this experiment is illustrated schematically in Figure 2. Ideal conditions are assumed: point-like source/receiver, scanning operated in free space, and an infinite perfectly reflective plane. It can be observed that the real experiment does not reproduce exactly these conditions because:

- scanning plane is made of solid wood;
- finite dimensions of scanning plane and metal plate;
- finite dimensions of the scanning head;
- structural parts are in range;
- operator's body is in range;

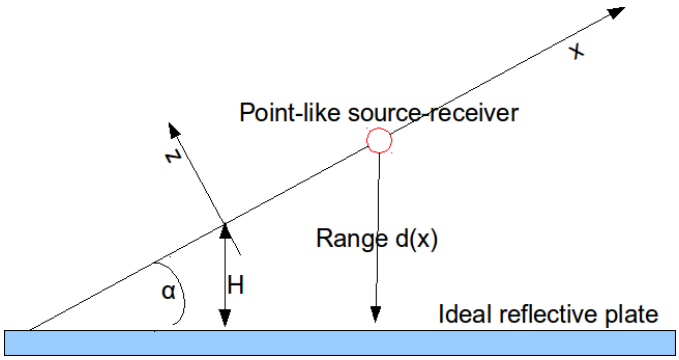

Figure 2: Schematic representation of a scan line.

These disturbance factors must be taken into account when comparing experimental data with the analysis and validation of a mathematical model. In a later section, a pre-processing method will be explained to separate the contribution to the system response of the metal plate reflection from the spurious ones.

III. SAMPLE IMAGES

Each surface scan produces a set of ten images consisting of five discrete frequencies at each of two channels with orthogonal polarization. The two output channels provide low frequency baseband signals that are sampled with 12 bits resolution. The scan lines are spaced at a fixed distance of 1cm while the spatial sampling along scanning lines is also 1cm, defining a grid of square pixels of $1x1cm^2$ on a $40x50cm^2$ image area.

The images used to fit the theoretical model on measured data (for parallel polarization only) are shown in Figure 3. These are, for each inclination α, the five images related to the parallel polarization at the nominal frequencies of 3.6, 3.7, 3.8, 3.9 and 4.0 GHz. Each image has in abscissa the scan line number and in ordinate the distance along the scan line.

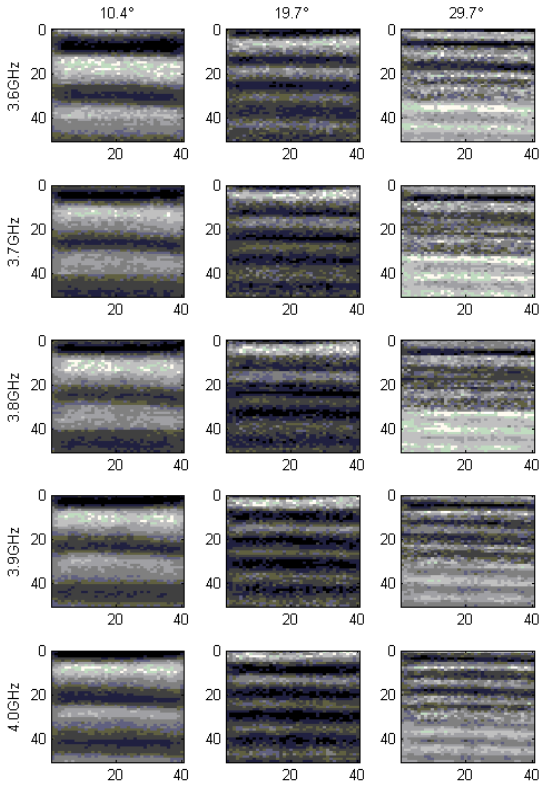

Figure 3: Parallel polarization sample images.

IV. PRE-PROCESSING

Because the scanning volume is in free air, reflection can occur also from structural parts, room parts and the operator's body. In the equipment response, these contributions are shown as oscillations with a wavelength that varies from 30cm to 60cm or more; for example, with reference to equation 2, a near wall that forms an angle of 5° with the scan line, give raise to an oscillation in the radar response at 4GHz with a wavelength of 0.075m/2*sin(5°)=0.43m.

Note that these values are larger than the expected distance of maxima and minima (zebra effect) appearing in the images for inclined plate reflector. Thus in these conditions the spurious signals can be decoupled from the response of the metal plate by subtraction from the measured signal.

In most cases the response from the complex surrounding environment can't be described with a proper mathematical model. A third order polynomial with the constraint that the spurious response must produce at most one complete oscillation in each scan has been used.

Because wanted and spurious signals are decoupled, the response from the metal plate is obtained by subtracting the fitted polynomial from the global response of the equipment. In the upper part of Figure 4 are shown the equipment response (BLUE) and the best-fitting third order polynomial (RED) while in the lower part is shown the result of the preprocessing. It can be seen that the preprocessed signal oscillates around zero as expected.

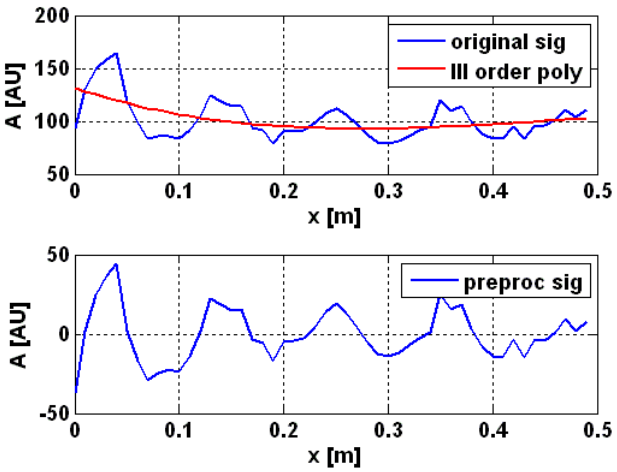

Figure 4: pre-processing on a scan line.

V. THEORETICAL MODEL

The RASCAN 4/4000 holographic radar records the amplitude of the interference signal corresponding to the probe position x individuated by a survey wheel. With reference to Figure 2, for each position x we can define a range d(x):

$$d(x) = H(x)\sin(\alpha) \quad (1)$$

Assuming a continuous wave (CW) operation at constant frequency f, we can define a round-trip phase variation ΔΦ (x,f) for a point-like probe operating in a medium with phase velocity v:

$$\Delta\Phi(x,f) = 2\cdot 2\frac{d(x)}{\lambda} = 2\left[\frac{2H}{\lambda'} - \frac{x}{\lambda'}\right]$$

$$\lambda' = \frac{\lambda}{2\sin(\alpha)} \quad (2)$$

The modified wavelength λ' depends on the tilt angle α and defines the distance between local maxima and minima that can be observed on the holographic images.

In the following table are reported the theoretical values of λ' for different values of α and assuming v=c and f=4GHz.

α [°]	λ' [m]
9	0.240
18	0.121
27	0.082

Considering the output of the holographic radar to be the baseband interference signal with amplitude variations A depending on ΔΦ (x,f), we obtain:

$$A(x,f) = \frac{A_0}{d(x)^2}\cos(\Delta\Phi(x,f)) \quad (3)$$

This function is used to model the holographic radar response for different values of x and α.

VI. FITTING PROCESS

To obtain values for the parameters that produces a curve that best fits the measured data, the program "fit" from *Curve fitting Toolbox* of MatLab (from *The MathWorks*) suite has been used. The expression to be fitted with the measured data is:

A0/(H+x*sin(ALPHA))^2* cos(2*pi*2*(H+x*sin(ALPHA))/LAMBDA + pi) (4)

In the argument of the cosine there appears a constant phase term π to account for the phase inversion due to the metallic surface of the reflective plate.

The parameters to be fitted (A0, LAMBDA and H) have been chosen because they are not known a-priori. In particular, the parameter A0 is unknown. The parameter LAMBDA is uncertain for two main reasons: the presence of the wooden scanning plane in the transmission path and an uncertainty of the real frequency emitted by the equipment.

The parameter H is also uncertain because scanning is a manual operation and thus subject to errors. Notice that an error ΔH on the parameter H generates an error of 2ΔH/LAMBDA on the phase. This means that, with a wavelength in air of – e.g. at frequency of 4GHz – 7.5cm, the fitting process can tolerate at most an error on H that is negligible with respect to 3.75cm.

Each scan of each image is elaborated with the fitting process described above. The scan line that gives the lower residual to measured data is chosen as representative of the set and its results are reported in Table 1. The residual (RES) is defined as the square sum of the errors to measured data.

VII. RESULTS

Table 1 summarizes the results of the elaboration of the set of five images from the parallel polarization channel.

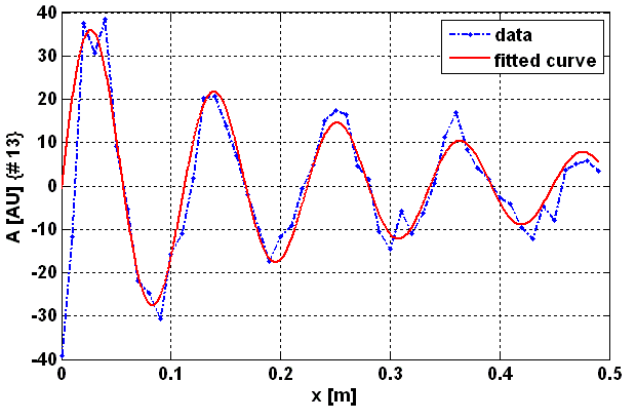

Figure 5

It can be noticed that the predicted frequencies have a good match with the nominal frequency set. Figure 5 shows the comparison, for the case of the image at 3.9GHz, parallel polarization and tilt angle 18°, between the measured (blue dashed line) and fitted (red solid line) data for the scan line that gave the best results in terms of residual. In the figure is also shown the ordinal number of the scan (13).

Table 1

α	CHAN	FREQ	RES	A0	LAMBDA	F	H
[]	[]	[GHz]	[AU]	[AU]	[m]	[GHz]	[m]
10.4	CROSS	3.6	9.99	1.48	0.083	3.6	0.14
10.4	CROSS	3.7	6.22	0.64	0.081	3.7	0.14
10.4	CROSS	3.8	5.95	0.17	0.073	4.1	0.1
10.4	CROSS	3.9	6.81	0.53	0.083	3.6	0.15
10.4	CROSS	4	6.21	0.3	0.080	3.7	0.12
10.4	PARALLEL	3.6	12.57	0.82	0.077	3.9	0.1
10.4	PARALLEL	3.7	9.32	0.62	0.084	3.6	0.13
10.4	PARALLEL	3.8	7.42	0.37	0.084	3.6	0.13
10.4	PARALLEL	3.9	5.46	0.4	0.081	3.7	0.12
10.4	PARALLEL	4	6.56	0.52	0.078	3.9	0.12
19.7	CROSS	3.6	8.32	1.04	0.079	3.8	0.14
19.7	CROSS	3.7	8.38	0.61	0.078	3.9	0.11
19.7	CROSS	3.8	7.4	0.28	0.072	4.2	0.11
19.7	CROSS	3.9	6.84	0.26	0.084	3.6	0.12
19.7	CROSS	4	4.77	0.1	0.077	3.9	0.11
19.7	PARALLEL	3.6	12.38	0.76	0.083	3.6	0.13
19.7	PARALLEL	3.7	8.99	1.1	0.078	3.8	0.12
19.7	PARALLEL	3.8	6.68	0.59	0.076	4.0	0.12
19.7	PARALLEL	3.9	4.47	0.63	0.076	4.0	0.12
19.7	PARALLEL	4	4.78	0.74	0.073	4.1	0.12
29.7	CROSS	3.6	7.08	0.21	0.083	3.6	0.12
29.7	CROSS	3.7	7.53	0.39	0.082	3.6	0.13
29.7	CROSS	3.8	7.22	0.28	0.075	4.0	0.1
29.7	CROSS	3.9	5.5	0.11	0.075	4.0	0.1
29.7	CROSS	4	4.22	0.12	0.086	3.5	0.14
29.7	PARALLEL	3.6	12.51	1.08	0.080	3.8	0.13
29.7	PARALLEL	3.7	11.86	1.22	0.078	3.8	0.13
29.7	PARALLEL	3.8	8.1	0.32	0.077	3.9	0.13
29.7	PARALLEL	3.9	5.72	0.44	0.076	4.0	0.13
29.7	PARALLEL	4	5.48	0.67	0.074	4.0	0.13

CONCLUSIONS

The experimental results introduced into the mathematical model for the inclined plate reflector show that the model fits well the underlying phenomenon. At the best fit, the values of estimated frequency (column F) shown in Table 1 are very close to the nominal value (column FREQ) for medium (19.7°) and high (29.7°) tilt angles, while it is less accurate for the low (10.4°) tilt angle. This effect is due to the smaller number of oscillations contained in the data set for images at low tilt angle.

This fact is also recognizable in Figure 3 where in the left (tilt angle α=10.4°) column are visible less then two oscillations while in the central column (tilt angle α=19.7°) there are four and in the right column (tilt angle α=29.7°) there are more then six.

Since continuous wave holographic radar does not record the time-of-flight as the impulse radar does, it is important to understand and to interpret the variation of the target depth in the holographic contrast images; for this aim has been developed and validated experimentally a simple mathematical model for a flat plate reflector at various inclinations.

More experiments with lossy materials and more complex shapes – e.g. with multiple sloping facets - will be required to enhance the mathematical model to be adequate for real target contour identification.

REFERENCES

[1] Inagaki, M., Windsor, C.G., Bechtel, T.D., Bechtel, E., Ivashov, S., and Zhuravlev, A. (2009) Three-Dimensional Views of Buried Objects from Holographic Radar Imaging. Proceedings of the Progress in Electromagnetics Research Symposium, PIERS 2009, August 18-21, Moscow, Russia, pp.284-287.

[2] Windsor, C.G, Bulletti, A., Capineri, L., Falorni, P., Inagaki, M., Bechtel, T.D., Bechtel, E., Zhuravlev, A., and Ivashov, S. (2009) Depth Information from Holographic Radar Scans. Proceedings of the Progress in Electromagnetics Research Symposium, PIERS 2009, August 18-21, Moscow, Russia, pp. 716-720

[3] Bechtel, T., Cassidy, M., Inagaki, M., Windsor, C., Capineri, L., Falorni, P., Bulleti, A., Valentini, S., Borgioli, G., Ivashov, S., Zhuravlev, A., Razewig, V., Vasiliev, I., Bechtel, E. (2009) The Donegal Sign Tree: A Local Legend Confirmed with Holographic Radar and 3-D Magnetics, Eos Trans. AGU, 90 (22).